Design of Non-overshooting PD and PID control systems for aerial vehicles
AE322 TERM PAPER

submitted by- **ANUNAY SHUKLA, RAMAN DHINGRA, RAJ PATEL & RITWIK SHANKAR**

Compiled 23/04/24

This paper involves the design of a non-overshooting PID controller for aerial vehicle systems. We examine two different approaches to achieve minimum overshoot in the systems. In the first implementation, the PID controller parameters are determined to reach a stable closed-loop system with a monotonically decreasing frequency response. Gain crossover frequency and phase iso-damping property are employed to choose an appropriate solution among the obtained solutions. For the second approach, three proposed conditions on the poles and zeros of the closed loop transfer function are analyzed. The results of implementing these conditions on an aeroplane plant are shown. GIT LINK for resources

1. INTRODUCTION

In the field of control engineering, achieving precision and stability is paramount. One significant challenge is non-overshooting control, especially in high-order systems with or without time delay, which is crucial for various applications, from circuit filters to aircraft control.

Traditional non-overshooting control methods often entail complex designs, leading to implementation hurdles. Additionally, current techniques focus on specific system types, limiting their applicability.

Our paper addresses the need for more straightforward non-overshooting control strategies, especially for high-order systems with time delays. We propose an approach grounded in fundamental principles, emphasizing stability and precision with minimal complexity.

A crucial aspect of our approach is the incorporation of gain crossover frequency and phase iso-damping criteria, which enable the selection of optimal controller parameters from a range of solutions. This ensures robust performance and resilience to uncertainties in the system.

Throughout our paper, we thoroughly analyze non-overshooting control principles, detail dominant pole structures, and provide practical examples. Our findings contribute to both theoretical understanding and practical implementation in engineering applications.

In subsequent sections, we explore foundational principles, delve into dominant pole structures, discuss placement methodologies, and present numerical examples. We conclude with a summary of critical insights and avenues for future research.

The necessity for precise altitude control in UAVs is paramount for various applications

- **Payload Stability:** Many fixed-wing Aircraft carry sensitive and expensive payloads that require stable flight conditions for optimal performance. Overshooting altitude targets can cause payload instability and substantial monetary damages.
- **Mission Effectiveness:** UAV missions often require precise altitude control to achieve specific objectives, such as aerial mapping, surveillance, or environmental monitoring. Minimizing overshoot ensures that the UAV maintains the desired altitude accurately, improving mission effectiveness and data quality.
- **Energy Efficiency:** Constantly adjusting altitude to correct overshoot consumes additional energy, reducing the UAV's endurance and flight range. By minimizing overshoot, UAVs can operate more efficiently, conserving battery power or fuel and extending mission duration.
- **Regulatory Compliance:** Many countries have regulations governing UAV operations, including altitude restrictions in certain airspace zones. Failure to maintain altitude within specified limits due to overshoot could result in regulatory violations and legal consequences for UAV operators.
- **User Experience:** For applications where UAV data or imagery is provided to end-users in real-time, such as live video streaming or emergency response operations, minimizing overshoot improves the user experience by delivering smoother and more stable footage.
- **Safety:** Overshooting altitude targets can lead to unsafe flight conditions, including potential collisions with obstacles or other aircraft. It can also cause passenger discomfort due to human-crewed flights.

As we are discussing multiple methods of finding the best PID, we will first test and simulate the first method for first-order

systems. This will be followed by solving airplane dynamics and using small perturbation theory to approximate the aircraft pitch's plant function. Then, using the dominant pole method, we will implement the algorithm to get appropriate PID values for a pitch control system of a UAV, which will minimize the overshoot at altitude.

2. BASIC PID CONTROLLER AND TIME DOMAIN RESPONSE

The basic PID controller has a transfer function that looks like:

$$G_c(s) = Kp + \frac{Ki}{s} + Kds \quad \textbf{(1)}$$

Kp, Ki, and Kd are the controller's proportional, integrator, and derivative gains. An example plant function has been taken as:

$$G_p(s) = \frac{3.45}{0.1s + 1} \quad \textbf{(2)}$$

Kp, Kd, and Ki have been varied randomly in 3 test cases to understand the time domain response of the closed-loop transfer function.

Test Cases	Kp	Ki	Kd
1	1	3	5
2	3	8	7
3	7	2	6

The three different time domain responses were plotted together, displaying rise time and maximum overshoot.

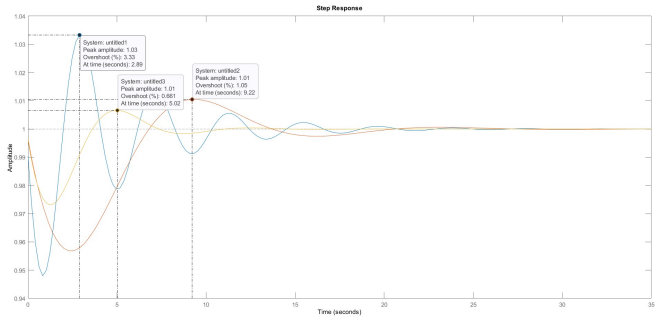

Fig. 1. Time Domain Response.

3. THE PROPOSED NON-OVERSHOOTING PID CONTROLLER

This study focuses on designing PID controllers to achieve a step response without overshoot for specific systems, including an aircraft plant. Our approach is guided by an empirical principle: systems with monotonically decreasing frequency responses tend to exhibit low overshoot in their step responses. Hence, we aim to select PID controller parameters that result in a closed-loop frequency response with a monotonically decreasing property.

Consequently, we derive inequalities concerning the PID controller parameters. Solving these inequalities numerically yields specific regions in the parameter space. This implies that various controllers could be designed to achieve a step response without overshooting.

From these controllers, we prioritize those that meet predefined criteria for gaining crossover frequency and phase damping. Iso-damping ensures that the phase of the loop gain frequency response remains flat around the gain crossover frequency. This characteristic enhances the robustness of the closed-loop system against gain uncertainties, ensuring that these uncertainties do not compromise the minimal overshoot property of the step response.

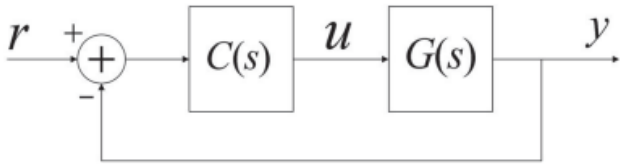

Fig. 2. The unit negative feedback control structure

Consider the unit negative feedback control structure in Figure 1. The controller C(s) (maybe a PD or PID controller) should be appropriately designed for a minimum phase plant G(s) so that the closed-loop system does not exhibit an overshoot in its step response. To accomplish this, it's essential to fine-tune the controller parameters to ensure that the magnitude of the closed-loop system's frequency response decreases consistently. Or

$$|H(j\omega_1)| < |H(j\omega_2)|, \quad for : \omega_2 < \omega_1 \quad \textbf{(3)}$$

where H(jω) is the frequency response of the closed loop system. The following remarks could be expressed by using relation (1).

- **Remark 1** Condition (1) means that when the frequency ω increases, the numerator of |H(jω)| increases smaller than its denominator.
- **Remark 2** Condition (1) applies to minimum phase plants. This requirement dictates that the closed-loop system must also be a minimum phase. Therefore, the plant and the controller must be designed to ensure the closed-loop system maintains minimum phase characteristics.
- **Remark 3** If condition (1) is met, a step response with minimal or negligible overshoot will be achieved. For instance, a second-order system featuring complex conjugate poles and a damping ratio falling within the range of (0.7, 1) fulfills condition (1) yet may exhibit a slight overshoot in its step response (below 5%). In practical control engineering scenarios, such minor overshoot may be deemed acceptable. Furthermore, condition (1) may lead to a step response with a marginal overshoot for transfer functions characterized by complex conjugate poles.

4. BASIC PRINCIPLES FOR NON-OVERSHOOTING

Here, three basic principles that the poles and zeros of the non-overshooting systems should follow are discussed.

Proposition 1: *A necessary condition for stable, rational, strictly proper transfer functions to have non-overshooting step responses is that the dominant poles of these transfer functions must be real.*

In control systems, achieving non-overshooting step responses is essential for stable and well-behaved performance.

For stable, rational, strictly proper transfer functions, a key condition for ensuring non-overshooting behavior is that the dominant poles must be real. When the dominant poles are real, the system's response to a step input approaches a final value without overshooting. Real dominant poles indicate exponential decay without oscillation, resulting in a stable response. This condition guarantees that the system settles at the desired value without oscillating around it, making it suitable for a wide range of practical control applications. It ensures a predictable and reliable system response, vital for control system design and implementation.

Proposition 2: *If the closed-loop transfer function with only one integrator in the forward path and unit feedback has a non-overshooting step response, both open-loop real zeros and real poles with the pole at origin excluded must lie to the left of the closed-loop dominant real poles.*

It can be concluded from Proposition 2 that when the open loop transfer function has RHP real poles, overshoots must exist in the step response of the closed loop. The dominant open loop real pole will determine the system's non-overshooting response speed. The condition that open-loop real zeros lie to the left of the closed-loop dominant real poles is necessary not only for closed-loop transfer functions to have a non-overshooting step response but also for closed-loop transfer functions to have a non-decreasing step response.

Proposition 3: *If* $p \geq 0, \alpha \geq 0, \beta \geq 0, k \geq 0, when p \leq \alpha, r \geq 1/2$, *transfer functions,* $G_1(s) = \frac{k}{(s+p)((s+\alpha)^2+\beta^2)}$ *and* $G_2(s) = \frac{k((s+\alpha)^2+r\beta^2)}{(s+p)((s+\alpha)^2+\beta^2)}$ *would have non overshooting step responses.*

Noted that no constraints are added to parameter β for transfer function G(s), therefore, it can be specified as a floating parameter in control system design.
Propositions 1 and 2 should be strictly followed for all non-overshooting systems, and Proposition 3 can be applied to non-overshooting control of third-order systems. These three propositions lay a foundation for designing non-overshooting systems with simple controllers.

5. DOMINANT POLE CONTROL STRUCTURE

Dominant pole control structure has a natural advantage for realizing non-overshooting control in that: (1) the dominance of the actual pole for non-overshooting control can be ensured; (2) dominant pole placement can be realized by simple controllers, such as PID controllers.
To ensure the dominance of the dominant poles, the ratio between the real parts of the non-dominant poles and that of the dominant poles, denoted as m, should satisfy that m ϵ [3, 5] or even m ϵ [3, 10]. Another fact is that complex conjugate poles are easily brought in by closed-loop control.
Another fact is that complex conjugate poles are quickly brought in by closed-loop control. Given the above problems, three poles, i.e., one actual pole $-\lambda\alpha$ and a pair of complex conjugate poles $-\alpha \pm \beta$, are adopted as dominant poles for non-overshooting control with $-\lambda < 1$ used to increase the robustness of non-overshooting control. The simple controllers used are mainly PD-PID controllers. The overall control structure is shown in Fig.3.

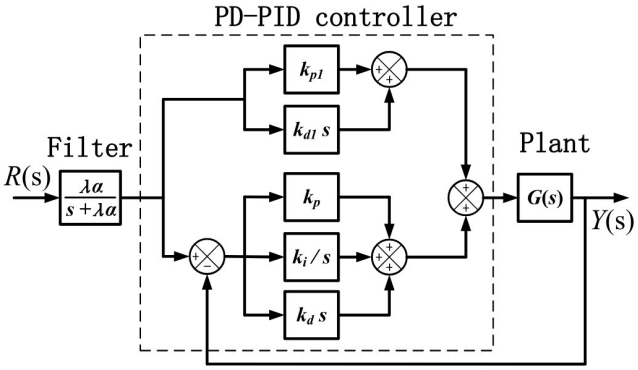

Fig. 3. Dominant pole control structure.

The advantage of the control structure in Fig. 3 is that three dominant poles can be designed independently. Dominant real pole $-\lambda\alpha$ can be offered by the first-order filter, while dominant complex poles $-\alpha \pm \beta$ can be designed in a PD-PID control loop. The transfer function of the non-overshooting dominant pole control structure is as follows,

$$\frac{Y(s)}{R(s)} = \frac{\lambda\alpha((k_d + k_{d1})s^2 + (k_p + k_{p1})s + k_i)N(s)e^{-\tau s}}{(s+\lambda\alpha)(sD(s) + (k_d s^2 + k_p s + k_i)N(s)e^{-\tau s})} \quad \textbf{(4)}$$

where $G(s) = N(s)e^{-\tau s}/D(s)$, and τ is a time delay.
The zeros brought in by the PD-PID controller and the closed-loop poles can be specified, respectively. By placing the zeros to the non-dominant poles close to the dominant complex poles, a system with a faster response can be designed as the dominant complex conjugate poles can be placed even further from the virtual axis. Note that the Dominant pole control structure in Fig. 2 can be further simplified without using a first-order filter since the PD-PID control loop can offer all three dominant poles.

A. Dominant pole placement

This section introduces the dominant pole placement method, which can place two poles to the specified points $-\alpha \pm \beta$ and make other non-dominant poles far away from these two poles. The characteristic equation of the PD-PID loop is as follows,

$$F(s) = sD(s) + (K_d s^2 + K_p s + K_i)N(s)\exp(-\tau s) \quad \textbf{(5)}$$

As $-\alpha \pm j\beta$ are two known roots of Eq. (19), two equations can be found when substituted into Eq. (19). Suppose that kp is a known variable; then kd and ki can be expressed by kp,α and β as follows:

$$k_i = \frac{\alpha^2+\beta^2}{2\alpha}k_p + (\alpha^2+\beta^2)A \quad \textbf{(6)}$$

$$k_d = \frac{1}{2\alpha}K_p + B \quad \textbf{(7)}$$

Where,

$$A = \frac{1}{2\alpha}Re(\frac{-1}{G(-\alpha+\beta j)}) + \frac{1}{2\beta}Im(\frac{-1}{G(-\alpha+\beta j)}) \quad \textbf{(8)}$$

$$B = -\frac{1}{2\alpha}Re(\frac{-1}{G(-\alpha+\beta j)}) + \frac{1}{2\beta}Im(\frac{-1}{G(-\alpha+\beta j)}) \quad \textbf{(9)}$$

Re(·) and Im(·) are functions of finding the real and imaginary part of a complex number correspondingly

Computers can calculate the values of A_11, A_21, and B_2. Thus, $-x_1$ and $-x_2$ can be solved after acquiring the value of X_1 and X_2 which can be solved as follows :

$$\begin{bmatrix} X_1 \\ X_2 \end{bmatrix} = \begin{bmatrix} A_{11}\ A_{12} \\ A_{21}\ A_{22} \end{bmatrix}^{-1} \begin{bmatrix} B_1 \\ B_2 \end{bmatrix} \quad \textbf{(10)}$$

Finally, according to pole-zero cancellation, parameters K_{d1} and K_{p1} can be determined by

$$k_{p1} = -\frac{k_i(x_1 + x_2)}{x_1 x_2} - k_p \quad \textbf{(11)}$$

$$k_{d1} = \frac{k_i}{x_1 x_2} - K_d \quad \textbf{(12)}$$

6. UAV PITCH CONTROL MODEL

The motion of an Unmanned Aerial Vehicle (UAV) is governed by two sets of equations: longitudinal and lateral equations. Longitudinal equations describe the motion of an aircraft in the pitching plane under steady-flight conditions, while lateral equations describe motion about the lateral plane under steady-flight conditions. This section describes the modeling of the pitch control longitudinal equation of a UAV. The longitudinal dynamics system is analyzed, and the transfer function and state equation are derived. The pitch control system is represented in Fig. 4, where X_b, Z_b represents the aerodynamic force components. θ, δ_e represents the pitch angle and the elevator deflection angle.

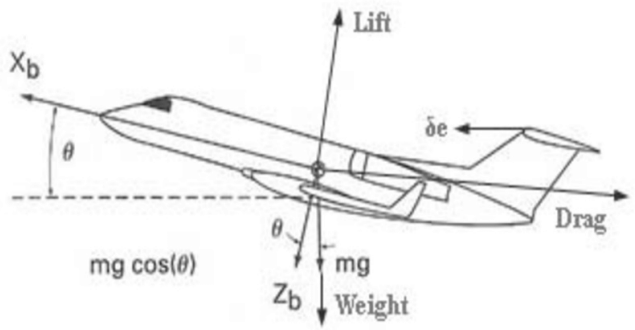

Fig. 4. Pitch Dynamics of a UAV.

Fig 5. shows the forces, moments, and velocity components in the body-fixed coordinate of the aircraft system.

Before modeling the pitch dynamics, a few assumptions were made to simplify the analysis. First, the aircraft is in steady state cruise at constant altitude and velocity, thus the thrust and drag cancel out and the lift and weight balance out each other. Second, the change in pitch angle does not change the speed of an aircraft under any circumstance.

The following dynamical equations are determined.

$$X - mgS_\theta = m(\dot{u} + qv - rv) \quad \textbf{(13)}$$

$$Z + mgC_\theta C_\phi = m(\dot{w} + pv - wu) \quad \textbf{(14)}$$

$$M = I_y\dot{q} + rq(I_x - I_z) + I_{xz}(p^2 - r^2) \quad \textbf{(15)}$$

The equations (10), (11), and (12) are linearized using the small

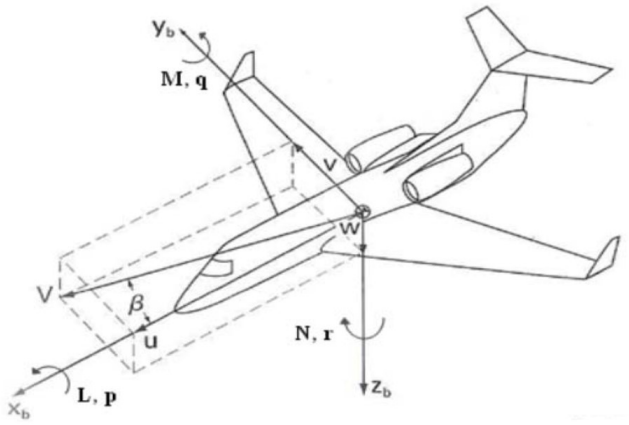

Fig. 5. Representation of forces and moments on the UAV.

disturbance theory. A perturbation is added to the variables as shown below:

$$u = u_o + \Delta u, \quad v = v_o + \Delta v, \quad w = w_o + \Delta w \quad \textbf{(16)}$$

$$p = p_o + \Delta p, \quad q = q_o + \Delta q, \quad r = r_o + \Delta r, \quad \delta = \delta_o + \Delta\delta \quad \textbf{(17)}$$

$$X = X_o + \Delta X, \quad M = M_o + \Delta M, \quad Z = Z_o + \Delta Z \quad \textbf{(18)}$$

The reference flight condition is assumed to be symmetric, and the propulsive forces are assumed to be constant, implying,

$$v_o = p_o = q_o = r_o = \phi_o = \psi_o = w_o = 0 \quad \textbf{(19)}$$

After linearization, the following equations are obtained,

$$(\frac{d}{dt} - X_u)\Delta u - X_w\Delta w + (gcos\theta_o)\Delta\theta = X\delta_e\Delta\delta_e \quad \textbf{(20)}$$

$$-Z_u\Delta u + [(1 - Z_w)\frac{d}{dt} - Z_w]\Delta w - [(u_o + Z_q)\frac{d}{dt} - gsin\theta_o]\Delta\theta = Z_{\delta e}\Delta\delta_e \quad \textbf{(21)}$$

$$-M_u\Delta u - [M_w\frac{d}{dt} + M_w]\Delta w + [\frac{d^2}{dt^2} - M_q\frac{d}{dt}]\Delta\theta = M_{\delta e}\Delta\delta_e \quad \textbf{(22)}$$

If the change in pitch rate is represented by Δq, it implies that the change in pitch rate is the first derivative of the pitch angle,

$$\Delta q = \Delta\frac{d}{dt}\theta \quad \textbf{(23)}$$

Taking the Laplace Transform of both sides of eq. (11),

$$\Delta q(s) = s\Delta\theta(s) \quad \textbf{(24)}$$

The transfer function of the aircraft pitch dynamics can be obtained as the Laplace Transform ratio of the change in pitch angle to the change in elevator angle,

$$\frac{\Delta\theta(s)}{\Delta\delta_e(s)} = \frac{1}{s}\frac{\Delta q(s)}{\Delta\theta(s)} \quad \textbf{(25)}$$

The transfer function of the pitch control system can be obtained as the Laplace Transform of the change in pitch angle to the shift in elevator angle based on eq.(13)

$$\frac{\Delta\theta(s)}{\Delta\delta_e(s)} = \frac{1}{s}[\frac{-(M_{\delta e} + \frac{M_\alpha Z_{\delta e}}{u_o})s - (\frac{M_\alpha Z_{\delta e}}{u_o} - \frac{M_{\delta e}Z_\alpha}{u_o})}{s^2 - (M_q + M_\alpha + \frac{Z_\alpha}{u_o})s + (\frac{Z_\alpha M_q}{u_o} - M_\alpha)}] \quad \textbf{(26)}$$

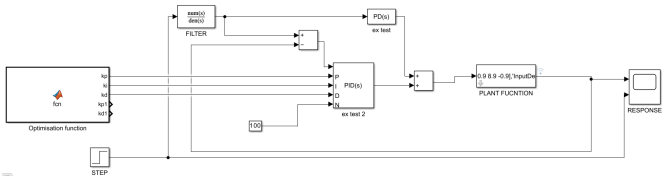

Fig. 8. CLOSED LOOP PITCH CONTROL SYSTEM of UAV

By substituting the longitudinal stability derivatives parameters values in eq.(22), the simplified transfer function is assumed as a 3rd order system:

$$G(s) = \frac{\Delta\theta(s)}{\Delta\delta_e(s)} = \left(\frac{1}{s^3 + 19.92s^2 + 145.94s + 467.4}\right) \quad \textbf{(27)}$$

7. MATHEMATICAL MODEL OF UAV AND ITS RESPONSE

The longitudinal transfer function of this model, by using the steering inertia model transfer function, can be estimated using equation (17)

The transfer function with a time delay is given by:

$$G(s) = \frac{1}{s^3 + 19.92s^2 + 145.94s + 467.4} e^{-.2s} \quad \textbf{(28)}$$

The longitudinal motion of the UAV can then be investigated using the transfer function depending on controller requirements.

Non-overshooting control of such a complex plant model, especially with time delay, is rigid for simple PID controllers. Suppose the dominant poles of the inner PD-PID control loop are set to be −1.0000 ±1.000j, let m = 3, and 2 more poles are allowed to exist inside a closed curve. Kp ϵ (1.71, 5.52) can be found to satisfy dominant pole placement. For simplicity, we take kp=2.

```
alpha=1;
beta=1;
kp=2;
A=1/(2*alpha).*real(-1./gpoletest(-1*alpha+beta*1i))+1/(2*beta).*imag(-1./gpoletest(-1*alpha+beta*1i));
B=-1/(2*alpha).*real(-1./gpoletest(-1*alpha+beta*1i))+1/(2*beta).*imag(-1./gpoletest(-1*alpha+beta*1i));
ki=(alpha^2+beta^2)/(2*alpha)*kp-(alpha^2+beta^2)*A;
kd=1/(2*alpha)*kp+B;
```

Fig. 6. Matlab code to get kp and kd parameters

where the transfer function is taken as 'politest,' which is

```
function y=gpoletest(s)
    y=1.*exp(-.2*s)/((s^2+s+9).*(s-.1));
end
```

Fig. 7. TF of the system

If kp = 2 is chosen, then ki = 0.2942 and kd = −5.8861 can be obtained by Eq.(6) and Eq.(7).d Two unknown poles close to −1.0000 ±1.000j can be determined by method given in subsection "calculating non dominant poles".We get k_{p1} and k_{d1} as −1.2562 and 7.6042. Parameter λ is set to be 0.98. The final system is given below. The responses for a magnitude step input are given below

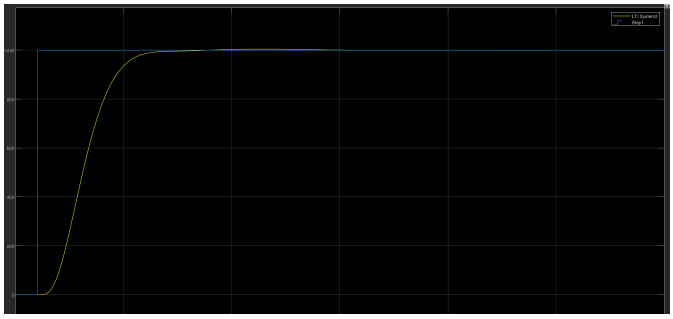

Fig. 9. Step response for our UAV model

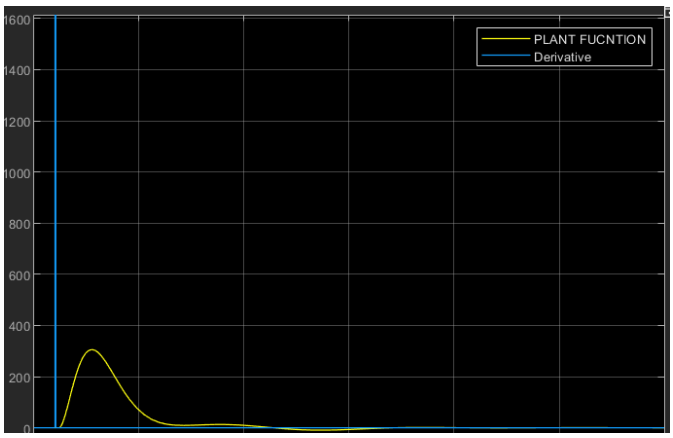

Fig. 10. Impulse response

No controller can have 0% overshoot. So we zoom further on the step input for in-depth analysis.

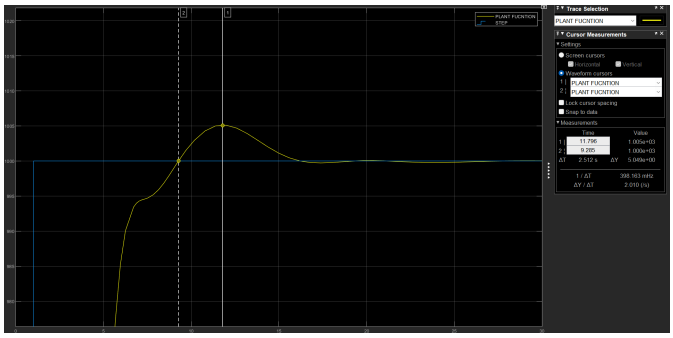

Fig. 11. Zoomed in image showing rise time

The rise time comes out to be approximately 9.285 s, and the overshoot is five units Maximum overshoot= 5/1000*100= **0.5%**, which is an excellent approximation on minimizing and neglecting the overshoot.

REFERENCES

1. Huanchao Du, Bobo Feng, Jieshi Shen, and Dan Li. Design of simple nonovershooting controllers for linear high order systems with or without time delay. *Scientific Reports*, 14(1):877, 2024.
2. Alfred E Onuora, Christian C Mbaocha, Paulinus C Eze, and Valentine C Uchegbu. Unmanned aerial vehicle pitch optimization for fast response of elevator control system. *International Journal of Scientific Engineering and Science*, 2(3):16–19, 2018.

3. Mohammad Tabatabaei and Reza Barati-Boldaji. Non-overshooting pd and pid controllers design. *Automatika: časopis za automatiku, mjerenje, elektroniku, računarstvo i komunikacije*, 58(4):400–409, 2017.
4. N Wahid, N Hassan, MF Rahmat, and S Mansor. Application of intelligent controller in feedback control loop for aircraft pitch control. *Australian Journal of Basic and Applied Sciences*, 5(12):1065–1074, 2011.